MRS Advances © 2017 Materials Research Society
DOI: 10.1557/adv.2017.237

Inkjet-Printed Flexible Active Multilayered Structures

Charles Trudeau[1, 2], Martin Bolduc[2], Patrick Beaupré[2], Patrice Topart[2], Christine Alain[2], Sylvain Cloutier[1]

[1]Department of Electrical Engineering, École de Technologie Supérieur, 1100 Notre-Dame Ouest,
Montréal, QC, Canada H3C 1K3
[2]Institut National d'Optique, 2740 Einstein Street,
Québec, QC, Canada G1P 4S4

ABSTRACT

Active inkjet materials are invoked in the fabrication of optoelectronic devices. These types of multilayer assemblies contain a variety of commercially available ink formulations. It is envisioned that a dielectric SU-8 material can be used in a FET-like structure to form an interlayer between conductive silver and semi-conductive MWCNT-doped PEDOT:PSS ink layers. These printed structures may be fabricated onto a polyimide based flexible substrate, for instance. These structures are a starting point for offering valuable information on layer-on-layer printing interactions and interface problematics within a complete inkjet device fabrication.

INTRODUCTION

Inkjet printing is a promising technology for flexible multilayer active devices printing. When using harsh or expensive materials for devices fabrication, this selective additive process becomes very advantageous due to the reduced amount of wastage and is very ecofriendly when compared to alternative fabrication processes or even other printing processes. Inkjet printing also allows for the use of most materials for device substrates as long as they offer a non-porous printing surface and can withstand every post- and/or pre-printing processes which are performed during the device fabrication steps.

Inkjet printing is a very mature technology, it is the advances in ink formulation that has made this process viable for device fabrication. A wide range of conductive, dielectric and more recently organic semiconducting inks have been made commercially available by various companies, these inks have made it possible to print simple multilayered active device architectures [1, 2].

Most multilayered device fabrication follow a similar layer by layer flow process. Starting with surface treatments of the printing substrate which can include underlying printed layers for printing subsequent layers. These treatments can take the form of hydrophilic-phobic surface treatments or surface cleaning processes for instance. In the following step, the layer is printed using previously optimized printing parameters to form a homogeneous layer of wanted characteristics. Once the layer is printed, post processes, such as annealing or layer activation, are performed to transform the ink in its final state [3, 4]. This flow process then repeats itself, for each subsequent layer until the device is fully printed. In this work, the effects of the printing parameters will be investigated, post- and pre-printing processes and their effects will be explored, and finally simple active multilayered device structures will be printed and investigated.

EXPERIMENT

A Ceradrop F-Series is used throughout this work for all printing purposes, UV and NIR lamps are available in-situ for optical post-printing processes. Hydrophilic surface plasma treatments were performed using a PlasmaTherm Unaxis 790 Plasma Etch system, and optical post-printing processes were performed using the in-situ UV and NIR lamps available on the Ceradrop F-Series printer. Characterization of liquid contact angles are obtained using an optical microscope for image acquisition and ImageJ for processing and extraction of contact angle measurements. Surface energies including both polar and dispersive components are calculated using the Owens/Wendt method with water, diodomethane, formamide and glycerol as test liquids. All layer thickness are measured using a Bruker 3D NPFLEX interferometry microscope system. SEM images are taken using a Hitachi S-3400N Scanning Electron Microscope system. All resistivity and sheet resistivity measurements are obtained using a conventional 4-point-probe.

In this work, printing parameters are optimized for four chosen inks. The following Ag nanoparticle inks are used for conductive layer formation: DGP 40TE-20C from ANP and Metalon JS-B40-G from Novacentrix. XP PriElex, a SU-8 formulation from MicroChem is used for insulator/dielectric layer formation. Finally, Poly-Ink HC, a MWCNT doped PEDOT:PSS formulation from Poly-Ink is used for active semiconductor layer formation. 0.002" thick Kapton® Polyimide film was used as the flexible printing substrate for this work.

RESULTS

Jetting Parameters

Stable ink jetting is the first essential step in the inkjet printing process. Both the jetting waveform sent to the nozzle and the choice of cartridge nozzle are important in obtaining a stable jet, an example of which is shown in Figure 1c). Figure 1d) illustrates a stable jetting sequence, it is important that the stable jet is void of ink trails and satellite drops at the printing distance, 500µm in this case. The ink trails and satellite drops are illustrated in Figure 1a) & b).

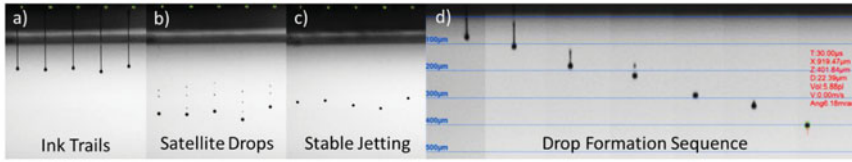

Figure 1 Inkjet drop analysis images taken with stroboscopic camera on CERADROP F-Series printer using ANP DGP 40TE-20C ink in Dimatix 1pL cartridge. a) Waveform used: 50V-3µm showing elongated ink trails. b) Waveform used: 35V-3µs showing few satellite drops at jetting distance. c) Waveform used: 22V-6µs showing stable drops at jetting distance. d) Waveform used: 22V-6µs showing stable drop formation.

An example of a jetting waveform is illustrated in of Figure 2b), the waveform intensity is defined as the highest intensity of the waveform and the time segment as the time spent at that intensity. This waveform was optimized for the stable jetting of each ink. In general higher waveform intensities tended to elongate the ink trails, often resulting in more satellite drops. A longer time segment generally resulted in less satellite drops and a more stable jet. Ink trails are present with most jetting parameters, however, only longer trails pose a problem in achieving a

stable jet, shorter tails are absorbed back into the drop before it reaches the printing distance as is shown in Figure 1d). The nozzle temperature has an effect on the ink viscosity which can affect the stability of the jet, in general an unstable temperature will result in an unstable jet. Too high of a temperature can cause premature evaporation of the ink solvent resulting in clogged nozzles, the nozzle temperature was kept constant between 26-35°C depending on the ink.

Figure 2a) illustrates the effects of the waveform intensity on the stable ink drop diameter, a higher waveform intensity resulted in a larger drop diameter. Figure 2a) also illustrates the change in drop diameter when either a Dimatix 1pL or 10pL cartridge is used. The change in drop diameter resulting from an increase in the waveform intensity from 22V to 50V equates to an increase in drop volume of close to 125%, a similar increase in drop volume can be calculated for the 10pL cartridges when compared to the 1pL cartridges.

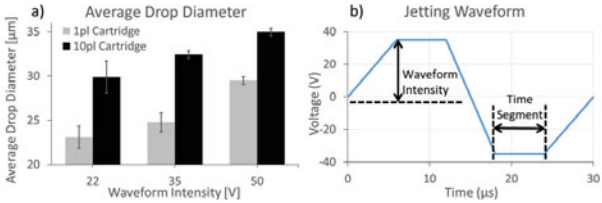

Figure 2 a) Effects of the waveform intensity and choice of Dimatix cartridge on the drop diameter. b) Example of jetting waveform sent to the nozzles' piezo transducers.

Printing Parameters

Once jetting parameters have been optimized and a stable jet is achieved for a given ink, the printing parameters can be investigated and optimized to achieve controllable homogenous printed layers. Two main parameters and their effects on the printed layer characteristics are presented here, the interpenetration of the ink drops and the temperature of the substrate.

The interpenetration of the ink drops on the substrate had a major impact on the printed layer thickness before any post-printing processes, this effect is shown in Figure 3. A greater degree of ink drop interpenetration results in more material being deposited per surface area and thus thicker layers. The measured thicknesses of the ANP ink layer for 0%, 25% and 50% drop interpenetration were 0.163±0.03µm, 0.287±0.12µm and 0.364±0.08µm, for the Novacentrix ink; 0.296±0.05µm, 0.445±0.11µm and 0.679±0.10µm, and finally, for the SU-8 ink; 0.575±0.08µm, 0.873±0.16µm and 2.56±0.17µm respectively. For homogenous, full layers, interpenetrations between 25% and 50% are needed as lower degrees of interpenetration can result in gaps within the layer. The choice of printing matrix also had effects on the homogeneity of the printed layer, printing matrices with drop arrangement offering the most coverage resulted in more homogeneous printed layers.

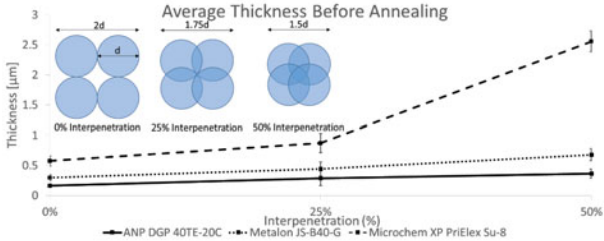

Figure 3 Effects of the interpenetration of the ink drops on the average thickness of the printed layers before any post-printing processes. Inset: Diagram of the layout of the ink drops with different interpenetration parameters.

The effects of the temperature on the layer thickness is shown in Figure 4. For the two silver inks and the PEDOT:PSS based ink an increase in substrate temperature resulted in thicker layers, for the SU-8 based ink, the opposite effect is seen. Two phenomenon are used to explain these tendencies. An increase in the substrate temperature can cause both a decrease in the liquid viscosity and a faster evaporation of the solvent which respectively increase and decreases the spread of the ink on the substrate [1] and is correlated to the thicknesses of the layers. Each ink solution is affected by these two phenomenon, the SU-8 ink material being more affected by the change in viscosity, and the other inks, by the accelerated solvent evaporation. The measured thicknesses of the ANP ink layer for chuck temperatures of 25°C, 40°C and 60°C were 0.298±0.09µm, 0.373±0.10µm and 0.450±0.04µm, for the Novacentrix ink; 0.421±0.09µm, 0.581±0.16µm and 0.803±0.20µm, for the PEDOT:PSS ink; 0.172±0.03µm, 0.176±0.02µm and 0.297±0.04µm, and finally, for the SU-8 ink, the measured thicknesses were 2.398±0.94µm, 1.984±0.87µm and 1.878±0.86µm respectively.

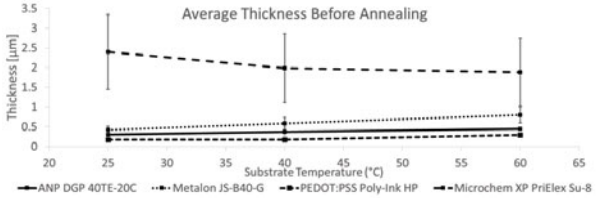

Figure 4 Effects of the substrate temperature on the average thickness of the printed layers before any post-printing processes.

Pre- & Post-Printing Treatments

Plasma surface treatments are performed to tailor the surface energy of the printing substrate and/or an already printed layer to allow printing on originally hydrophobic materials. Figure 5 illustrates the results from a 30W oxygen plasma treatment on a polyimide substrate, similar results were obtained for oxygen plasma with varying operating power as well as for argon plasma, on both polyimide and a SU-8 printed layer. It must be noted that although the achieved surface energies were similar for all hydrophilic plasma treatment parameters, the ageing properties of these processes are thought to differ greatly [5-7]. Since the plasma treatments are performed directly before printing, these effects were not investigated.

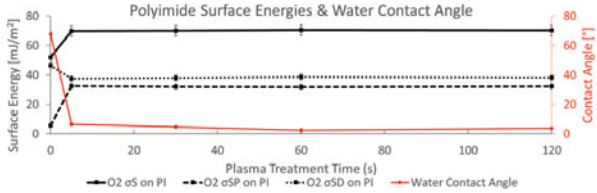

Figure 5 Substrate surface energy and water drop contact angle variation with 30W oxygen plasma treatment time performed using the PlasmaTherm Unaxis 790 Plasma Etch System.

For the case of the two silver inks, annealing must be performed to achieve conductive layers. Figure 6 illustrates the drop in resistivity when the two metal inks are annealed using the NIR lamp attached to the Ceradrop F-Series printer, the stated temperatures are measure using a thermocouple attached to substrate plate (chuck) during the NIR exposure. Final sheet resistivity of 2.6±0.28Ω/sq and 0.07±0.03Ω/sq were obtained for ANP's and Novacentrix's Ag inks respectively, the results for the Novacentrix's ink is in agreement with those stated by the ink supplier whereas the result from ANP's silver ink is one order of magnitude larger than stated by the supplier. Therefore only Novacentrix's ink was used for the multilayered structure printing.

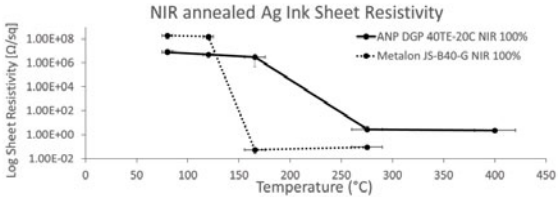

Figure 6 NIR annealing of ANP's and Novacentrix Ag inks using Ceradrop F-series' attached lamp. Temperatures measured using thermocouple on substrate plate.

Multilayer Structure Printing

Three fully-printed multilayered device structures were realized. Figure 7a) illustrates an antenna device structure comprising of Ag/SU-8/Ag layers on a polyimide substrate. Hydrophilic plasma treatments were used to treat the polyimide substrate before printing the first Ag layer and another plasma treatment was used to treat the SU-8 layer to allow the subsequent Ag layer to be printed, the second plasma treatment was done using argon plasma to avoid oxidation and degradation of the first Ag layer. The Ag layers were annealed using the NIR lamps after each layer was printed.

Figure 7b) illustrates a thermistor structure comprising of an active MWCNT doped PEDOT:PSS layer printed on top of Ag electrodes. Oxygen plasma was used to treat the polyimide before printing and NIR annealing was used to treat the printed Ag layer. Oven curing at 200 °C for 1 hour was needed to achieve an ohmic contact between the PEDOT:PSS and the Ag electrodes resulting in a final device resistance of 870Ω.

Figure 7c) illustrates a more generic multilayered device structure consisting of Ag/SU-8/PEDOT:PSS layers, oxygen plasma treatments were used both on the polyimide substrate prior to printing the PEDOT:PSS layer and on the printed SU-8 layer prior to printing the last Ag layer. NIR annealing was performed after printing the last Ag layer. Oven curing at 200°C for 1 hour was also perform on the final structure to provide better inter-layer adhesion.

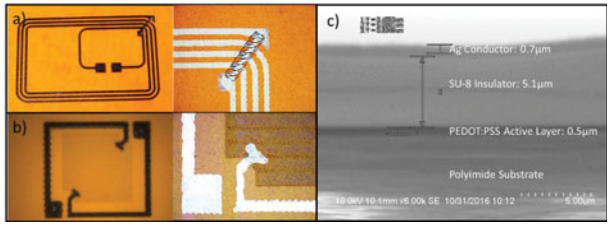

Figure 7 Three fully inkjet-printed device architectures. a) An antenna architecture comprising of Ag/Su-8/Ag layers. b) A thermistor structure comprising of Ag/PEDOT:PSS layers. c) SEM image of a generic multilayered structure comprising of Ag/SU-8/PEDOT:PSS layers.

DISCUSSION & CONCLUSION

Although the optimized printing and jetting parameters vary for each ink material, the general trends and effects are shown. The optimization of the jetting waveform is shown to be crucial for achieving stable jetting of ink drops, it is also an important controlling parameter for the size of the jetted ink drops. The printed layers characteristics are shown to be controlled by varying the interpenetration of the printed drops as well as the printing substrate temperature. It is interesting to see that this dependence can vary with the ink material. Hydrophilic pre-printing treatments are performed using either oxygen or argon plasma, this process was needed for printing on polyimide substrates and also for printing on previously printed SU-8 layers. Oxygen plasma was found to degrade and/or oxidize exposed printed Ag ink, therefore argon plasma was used whenever exposed printed Ag ink was present. Optical annealing processes were performed on the printed Ag inks, the NIR annealing process gave good results in terms of conductivity for one of the Ag inks but fell short for the other. Although this process was adequate for conductivity purposes, oven curing was still used on complete multi-layered structures to achieve good inter-layer contacts and interfaces. Three different multilayered device structures were printing on flexible substrates to validate the optimization of the whole printing process as well as the final interface quality between different printed layers.

REFERENCES

1. D. Sette, *Functional printing: from the study of printed layers to the prototyping of flexible devices* (Doctoral dissertation, Université de Grenoble, 2014).
2. W. Su, Q. Liu, B. Cook, and M. Tentzeris, *All-inkjet-printed microfluidics-based encodable flexible chipless RFID sensors.* (In Microwave Symposium (IMS), 2016 IEEE MTT-S International) pp. 1-4.
3. D. Kim, and J. Moon, Electrochemical and Solid-State Letters, 8(11), J30-J33 (2005).
4. J. West, J. Sears, M. Carter, and S. Smith, *Photonic sintering of silver nanoparticles: comparison of experiment and theory.* (INTECH Open Access Publisher, 2012) pp.173-188
5. S.J. Park, E.J. Lee, and S.H. Kwon, Bulletin of the Korean Chemical Society, 28(2), 188-192 (2007).
6. V. Jokinen, P. Suvanto, and S. Franssila, Biomicrofluidics, 6(1), 016501 (2012).
7. F. Walther, P. Davydovskaya, S. Zürcher, M. Kaiser, H. Herberg, A.M. Gigler, and R.W. Stark, Journal of Micromechanics and Microengineering, 17(3), 524 (2007).